

Research of Electromagnetic-Thermal Coupling Mechanism Based on a Physical Model of AlGaIn/GaN HEMTs

Xiaobin Luo, Weihua Yu, and Xin Lv

Lab of Microwave Communication and Electronic Systems, Beijing Institute of Technology, Beijing, 100081, China
Email: xiaobing53@126.com; ywhbit@bit.edu.cn; lvxin@bit.edu.cn

Abstract—A single-finger physical model of 180 nm gate-length and 75 μm gate-width AlGaIn/GaN HEMTs is described including lateral structure and vertical material parameters. The Farahmand Modified Caughey Thomas fitting function and the Monte Carlo model are used to express the 2DEG mobility in low and high field respectively. Then DC characteristics is simulated and the initial condition generated by self-heating effect is determined under DC bias. Electromagnetic-thermal (EM-T) coupling mechanism during the whole process is analyzed and the AlGaIn/GaN HEMT structure is calculated combining with equations in electromagnetic field, microelectronics and thermal field under different RF input signals. Finally, high frequency characteristics of the device is obtained. The result shows that the highest junction temperature is 126 $^{\circ}\text{C}$ under -2 V gate voltage, 25 V drain voltage and 16 dBm CW RF input signal. The current gain cutoff frequency (f_T), the maximum frequency of oscillation (f_{max}) and the maximum available power gain (MAG) at 40 GHz decrease 13%, 17% and 18%, respectively, at 16 dBm by contrasting to 8dBm.

Index Terms—physical model, AlGaIn/GaN HEMTs, mobility, electromagnetic-thermal coupling.

I. INTRODUCTION

AlGaIn/GaN HEMTs (High Electron Mobility Transistors) are on a great favor for high frequency and high power devices by researchers because of its advantages like wide band-gap, high electron drift velocity, high temperature resistant, high voltage resistant and radiation resistant. Along with rise of working frequency and diminishment of physical dimension of devices constantly, the HEMTs have started to be applied at millimeter-wave band [1], [2]. However, the making process shows its complexity and there are lots of structural and material parameters need to be adjusted. Therefore, semiconductor simulation technology is an indispensable method during designing AlGaIn/GaN HEMTs for its fast calculation and low cost in the research. In the paper, the Silvaco TCAD software and Comsol Multiphysics software are helpful to design the

HEMTs and simulate some characteristics which are related to device performance [3]-[5].

The main reason of application of GaN power devices being restricted in high frequency is that the 2DEG mobility of GaN is much lower than that of GaAs and InP materials, which has exceeded 2000 $\text{cm}^2/\text{V sec}$ at room temperature now [6]. For high frequency and high power devices, the thermal problem turns more and more important and it can not be ignored in the design no longer. The junction temperature of devices reaches too high, which is higher than 100 $^{\circ}\text{C}$ even 150 $^{\circ}\text{C}$ usually. So it leads the mobility declining sharply and deteriorates high frequency performance of devices seriously. In addition to self-heating effect brought by the high DC voltage, the RF input signal is also a key factor which can lead to temperature increasing. Based on such consideration, we propose a method by using electromagnetic-thermal (EM-T) coupling mechanism based on self-heating effect to analysis high frequency characteristics of AlGaIn/GaN HEMT devices under different input signals. The 2DEG mobility model in low field during the channel is associated with junction temperature and it becomes a link among multi-physics field. Thus, all of the contents have provided theoretical basis and guidance for researching GaN devices during millimeter-wave band.

II. PHYSICAL MODEL

A. Structural Parameters

The physical model structure of AlGaIn/GaN HEMT is shown in Fig. 1. The gate uses the classic "T" type structure with 180 nm gate-length, 75 μm gate-width, 200 nm gate-cap-length beside the source and 400nm gate-cap-length beside the drain. The thickness of the AlGaIn barrier layer is 20 nm in the structure. SiN is used as the passivation layer which thickness is 120 nm [7]. The distance between the source and the drain is 2.8 μm and the distance between the gate and the source is 0.6 μm [8]. SiC is selected as the substrate for its higher thermal conductivity compared to sapphire. The epitaxial layer is a 1.5 μm thickness GaN buffer layer and a 10 nm thickness GaN channel layer is on the buffer layer [9]. Then a 1 nm thickness AlN layer is inserted between the

Manuscript received March 9, 2013; revised April 24, 2013.
Corresponding author email: xiaobing53@126.com.
doi:10.12720/jcm.8.5.282-287

barrier layer and the channel layer to increase 2DEG concentration of the channel layer surface.

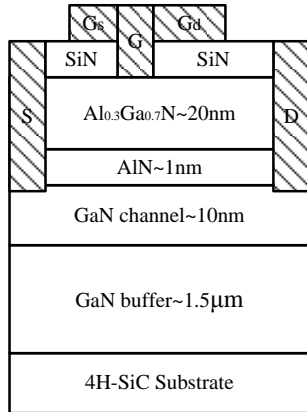


Figure 1. Physical structure of AlGaIn/GaN HEMTs

TABLE I. EMPIRICAL FITTING COEFFICIENTS OF LOW FIELD MOBILITY

A	B	C	D	E	F	M ₁	M ₂
0.66	-1.02	3.02	0.81	10 ¹⁷	-3.84	295	1500

TABLE II. EMPIRICAL FITTING COEFFICIENTS OF HIGH FIELD MOBILITY

VSATN	ECN	N1N	N2N	ANN
1.9×10 ⁷	220.9	7.2	0.8	6.2

Combined with actual process, the Al content of the barrier layer AlGaIn is set 0.3. All the layers are unintentional doped and the background doping concentration is 10¹⁵ cm⁻³. The values of spontaneous polarization of materials and piezoelectric polarization of the AlGaIn/GaN heterojunction can guarantee the 2DEG surface charge density reach 7×10¹² cm⁻². The contact resistances of the source and drain are both set 0.5 Ω·mm. And, the work function of the gate metal is set 4.8 eV.

B. Mobility Models

The GaN buffer layer has exhibited high resistance characteristics and the mobility is set 300 cm²/V sec. The channel layer surface has much high 2DEG mobility and we can use empirical models as the function to solve self-heating effect [10], [11].

To low field, the Farahmand Modified Caughey Thomas model has been used.

$$\mu_{n0}(T,N) = M_1 \left(\frac{T}{300}\right)^B + \frac{(M_2 - M_1) \left(\frac{T}{300}\right)^C}{1 + \left[\frac{N}{E \left(\frac{T}{300}\right)^F}\right]^{A(T/300)^D}}$$

Here, T and N represent junction temperature and doping concentration respectively. $A \sim F$, M_1 and M_2 are fitting coefficients. The 2DEG mobility at room temperature may be set 1500 cm²/V sec as well. All of the empirical fitting coefficients are shown in Table I.

To high field, the model based on Monte Carlo method has been used.

$$\mu_n(T,N,E) = \frac{\mu_{n0}(T,N) + VSATN \frac{E^{N1N-1}}{ECN^{N1N}}}{1 + ANN \left(\frac{E}{ECN}\right)^{N2N} + \left(\frac{E}{ECN}\right)^{N1N}}$$

where E represents electric field. All of the empirical fitting coefficients are shown in Table II.

III. DC CHARACTERISTICS

A. I-V and C-V Characteristics

According to above structure and material parameters, the Silvaco TCAD software is used to complete the whole simulation. The gate voltage is changed from -4 V to 1 V and the curves of $I_{ds}-V_{ds}$ are shown in Fig. 2. The channel of the device starts to enter on-state when the gate voltage is -4 V which is regarded as the threshold voltage. The curves are a little upturned in saturation zones and that reflects short channel effect brought by the short gate-length. The drain current begins to decline as increasing of the drain voltage in the saturation zone for self-heating effect when the gate voltage exceeds -1 V. When the gate voltage is 0V, the saturation drain current can reach 87 mA and the knee voltage is 5 V, that indicates strong depletion type characteristics of the HEMT device.

The curves of $I_{ds}-V_{gs}$ and g_m-V_{gs} are shown in Fig. 3. When the drain voltage is 10 V, the maximum transconductance is 410 mS/mm, and this peak value appears when the gate voltage is -2 V.

The curves of $C_{gs}-V_{gs}$ and $C_{gd}-V_{gs}$ are shown in Fig. 4. According to the calculation formula

$$f_T = \frac{g_m}{2\pi \cdot (C_{gs} + C_{gd})}$$

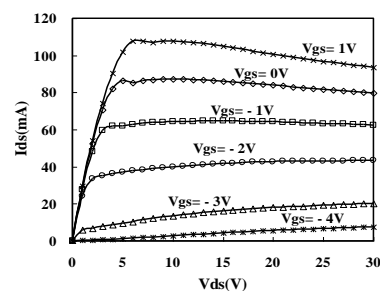


Figure 2. Curves of $I_{ds}-V_{ds}$

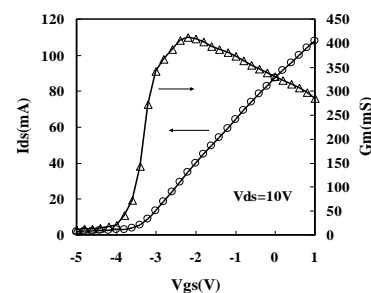


Figure 3. Curves of $I_{ds}-V_{gs}$ and g_m-V_{gs}

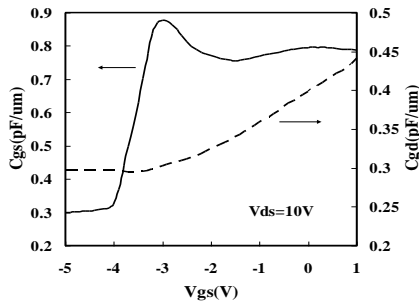


Figure 4. Curves of $C_{gs}-V_{gs}$ and $C_{gd}-V_{gs}$

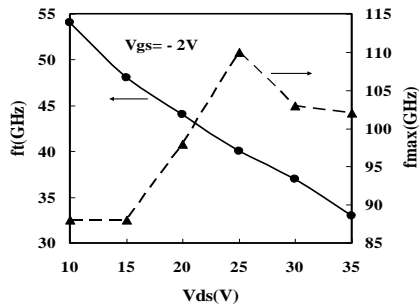


Figure 5. Curves of $f_T - V_{ds}$ and $f_{max} - V_{ds}$

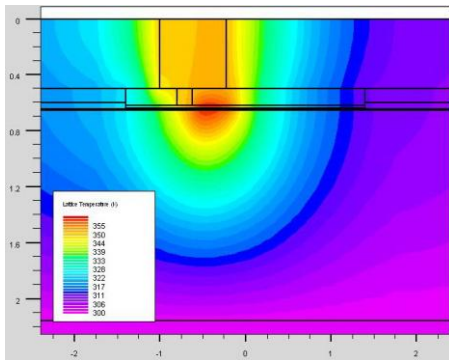


Figure 6. Temperature distribution of AlGaIn/GaN HEMTs under self-heating effect

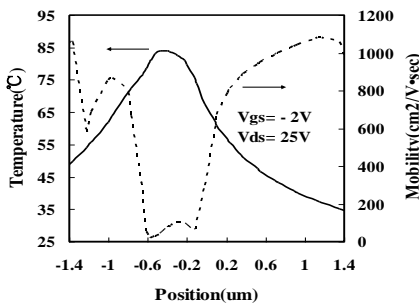


Figure 7. Temperature and mobility distribution in the channel under self-heating effect

The highest f_T is obtained when the gate voltage is -2V at last it means the best gate voltage has been found.

From Fig. 5 we can see that the f_T declines along with increasing of the drain voltage when the gate voltage keeps unchanged. The f_{max} varies as different drain voltage and the maximum is obtained fast when the drain

voltage is 25 V. So the best drain voltage has also been found. Thus, -2 V gate voltage and 25 V drain voltage can be selected as the DC bias when the device is operated as a power amplifier at Ka-band [12].

B. Self-heating Effect

In order to simulate the self-heating effect, the ambient temperature and original temperature of the base plate are both set 27 °C. When the gate voltage is -2 V and the drain voltage is 25 V, temperature distribution in the structure is shown in Fig. 6. The positions near the gate have higher temperature compared with others and the channel below the gate-cap beside the drain has the highest temperature resulted from self-heating effect [13].

Fig. 7 shows temperature and mobility distribution in the channel. The highest junction temperature may reach 85 °C. The mobility during all positions is lower than the initial value apparently under self-heating and strong electric field effect, especially almost declining to zero below the gate. The reduction of mobility will lead to the channel resistance increasing sharply and then make frequency characteristics go bad rapidly.

IV. EM-T COUPLING

A. EM-T Coupling Mechanism

When the AlGaIn/GaN HEMT device is inputted RF signals, electromagnetic field distribution is formed inside the device structure. Then the dissipation power is generated through semiconductor materials and heat conduction occurs during the structure with the power as the heat resource. So temperature during all positions will change and the mobility in the channel will also change, that can lead to electrical conductivity different from origin state. At this time, electromagnetic field distribution will be calculated again until reaching steady state finally. Meanwhile, we can obtain temperature distribution at steady state [14-15]. The whole process is simulated by using the Comsol Multiphysics software.

Equations used for EM-T calculation are shown below:

Maxwell equations

$$\nabla \times H = J + \frac{\partial D}{\partial t}$$

$$\nabla \times E = -\frac{\partial B}{\partial t}$$

$$\nabla \cdot D = \rho, \quad \nabla \cdot B = 0$$

Constitutive equations

$$D = \epsilon_0 \epsilon_r E$$

$$B = \mu_0 \mu_r H$$

$$J = \sigma E$$

Poisson equation

$$\nabla \cdot (\epsilon_0 \epsilon_r \nabla \psi) = -q(p - n + N_D^+ - N_A^+)$$

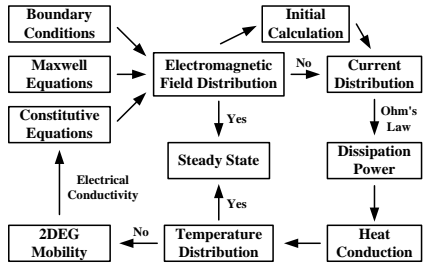


Figure 8. Flow chart of EM-T coupling mechanism

Carrier continuity equations

$$\nabla \cdot J_n - q \frac{\partial n}{\partial t} = -q(G - R)$$

$$\nabla \cdot J_p + q \frac{\partial p}{\partial t} = q(G - R)$$

Carrier current relation formulas

$$J_n = -q(\mu_n n \nabla \psi - D_n \nabla n)$$

$$J_p = -q(\mu_p p \nabla \psi + D_p \nabla p)$$

Heat conduction equations

$$\nabla \cdot [k(T) \nabla T] = \rho C \frac{\partial T}{\partial t} + P_{diss}$$

$$P_{diss} = JE$$

EM-T coupling mechanism is shown in Fig. 8.

B. EM-T Simulation

The Based on the DC bias above, we input the 10dBm CW signal for the device at 40 GHz. The rise of temperature distribution cross section diagram obtained through EM-T coupling mechanism is shown in Fig. 9 at steady state. We can assume that EM-T coupling characteristics is unchanged along as the gate-width direction for the reason that the 75 μm gate-width meets the principle that the phase difference is no more than π/16 and the propagation loss can be ignored. In the diagram, the temperature below the gate begins to increase and this phenomenon will be more obvious if the input signal rises. So the final junction temperature should be determined under the common action of DC bias and RF signals. And EM-T coupling is an effective method to analyze temperature distribution generated from RF signals.

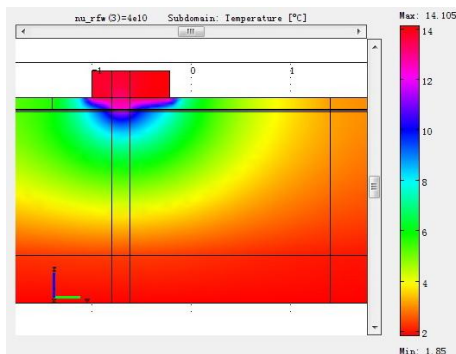


Figure 9. Rise of temperature distribution calculated by EM-T coupling at steady state

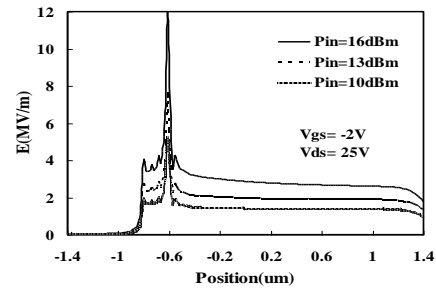


Figure 10. Electric field distribution in the channel

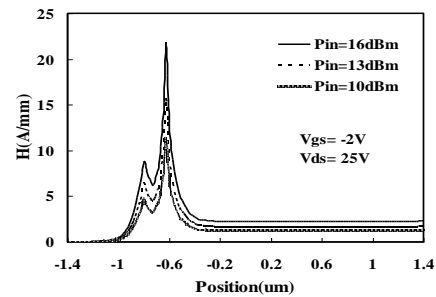


Figure 11. Magnetic field distribution in the channel

Electric and magnetic field distribution in the channel at steady state can be got through altering RF input signals, shown in Fig. 10 and Fig. 11 respectively. It goes without any slightest question that they both increase as the signal turns higher and the amplitude under the 16 dBm signal is two times of that under 10 dBm. We can know that electric field is not uniform in the channel especially higher below the gate and may generate higher dissipation power which can lead temperature rise fast. Magnetic field is also the highest below the gate because the area from the gate to the ground on back of the substrate is the RF signal input port and the AC signal forms strong alternating magnetic field.

Temperature and mobility distribution in the channel at steady state are shown in Fig. 12 and Fig. 13 respectively. The maximum temperature reaches 126 °C when the input signal is 16 dBm and this temperature is far higher than that under DC bias only. The mobility in the channel will go on turning lower as the RF input signal increases and the highest value may decrease to be lower than 800 cm²/V sec at 16 dBm.

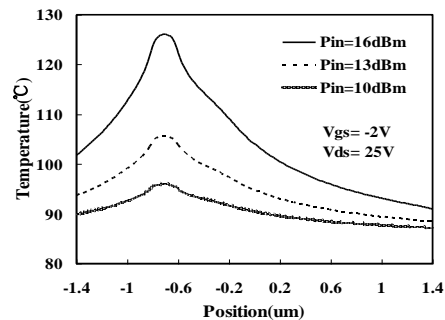


Figure 12. Temperature distribution in the channel

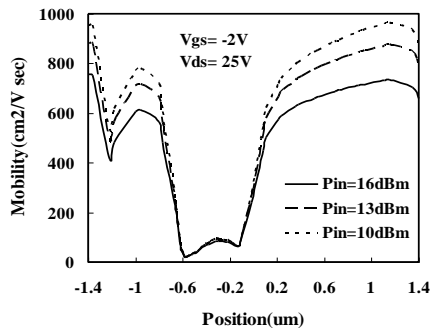


Figure 13. Mobility distribution in the channel

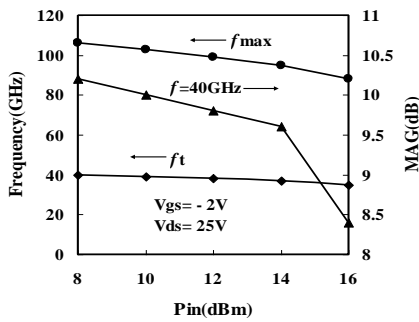


Figure 14. Frequency and gain characteristics under different input signals

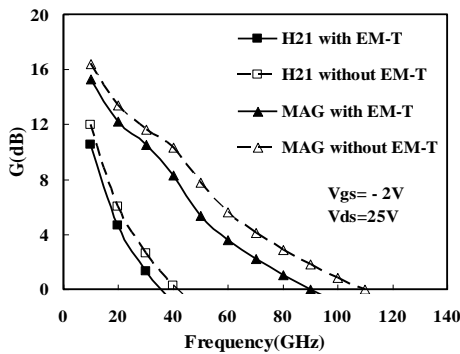


Figure 15. Current and power gains with and without EM-T coupling at 16dBm

C. High Frequency Degeneration

Fig. 14 shows that the f_T and f_{max} are 40GHz and 106GHz when the input signal is 8dBm and the maximum available power gain (MAG) is 10.2dB at 40GHz. As the input signal increasing, the f_T will decline a little, but the f_{max} and the MAG at 40 GHz will drop obviously. The f_T and f_{max} are 35GHz and 88GHz when the input signal is 16dBm and the MAG is 8.4dB at 40GHz. The decline rate is 13%, 17% and 18% respectively. Here, 16dBm is still assumed as the small signal and large signals will be also affected by EM-T coupling effect accordingly. Fig. 15 shows that the f_T and f_{max} considering EM-T coupling effect are lower than those ignoring EM-T coupling effect at 16dBm and this is an important reason that the actual gain of AlGaIn/GaN HEMTs always drops when working as power amplifiers.

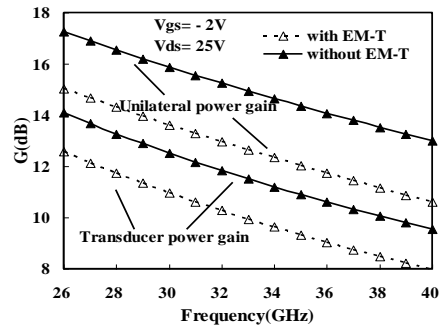


Figure 16. Power gains with and without EM-T coupling at 16 dBm during Ka-band

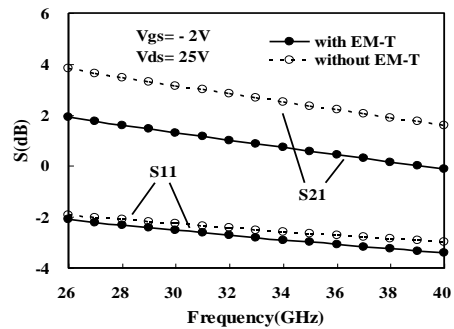


Figure 17. S-parameters with and without EM-T coupling at 16 dBm during Ka-band

We can also see that the unilateral power gains, the transducer power gains and S-parameters all decline sharply at 16 dBm during Ka-band in Fig. 16 and Fig. 17. This phenomenon can affect accuracy of parametric modeling from the physical structure model if RF input signals have not been analyzed properly by taking advantage of the relationship between electromagnetic field and thermal field.

V. CONCLUSION

The AlGaIn/GaN HEMT has been designed and simulated through structural modeling while DC and high frequency characteristics are both obtained by taking advantage of the Silvaco TCAD software. We have described the method of EM-T coupling mechanism and analyzed thermal and high frequency degeneration characteristics of the physical model by using the Comsol Multiphysics software. The final result shows that the highest junction temperature is 126 °C under -2 V gate voltage, 25 V drain voltage and 16dBm CW RF input signal. The f_T , f_{max} and MAG at 40 GHz decreases 13%, 17% and 18% respectively at 16 dBm by contrasting to 8dBm. The method contributes to get reasonable trend prediction and become an effective route for designing millimeter-wave GaN devices. In addition, multi-physics coupling has become indispensable idea in many fields and the method in the paper has provided application of reference for interdisciplinary science.

ACKNOWLEDGEMENT

The authors would like to thank the help of engineers from the Silvaco Company and the CnTech Corporation. This work was supported by the National “973” Project of China (No. 2010CB327505).

REFERENCES

[1] R. S. Pengelly, S. M. Wood, J. W. Milligan, S. T. Sheppard, and W. L. Pribble, “A review of GaN on SiC high electron-mobility power transistors and MMICs,” *IEEE Trans. Microw. Theory & Tech.*, vol. 60, no. 6, pp. 1764-1783, June 2012.

[2] D. F. Wang, T. T. Yuan, K. Wei, X. Y. Liu, and G. G. Liu, “Design and implementation of Ka-band AlGaIn/GaN HEMTs,” *Journal of Infrared and Millimeter Waves*, vol. 30, no. 3, pp. 255-259, June 2011.

[3] J. L. Chen, D. Wang, and W. B. Zhao, “A task scheduling algorithm for hadoop platform,” *Journal of Computers*, vol. 8, no. 4, pp. 929-936, April 2013.

[4] Q. Wu and L. Y. Zhang, “New efficient hierarchical identity-based signature,” *Journal of Computers*, vol. 8, no. 3, pp. 803-810, March 2013.

[5] F. Xiao, Y. J. Zhou, J. X. Zhou, H. L. Zhu, and X. X. Niu, “Security protocol for rfid system conforming to epc-c1g2 standard,” *Journal of Computers*, vol. 8, no. 3, pp. 605-612, March 2013.

[6] X. L. Wang, C. M. Wang, G. X. Hu, Z. Y. Ma, *et al.*, “High quality AlGaIn/GaN HEMT materials grown on sic substrates,” *Journal of Semiconductors*, vol. 28, Supplement, pp. 402-406, September 2007.

[7] J. M. Tirado, J. L. S. Rojas, and J. I. Izpura, “Trapping effects in the transient response of AlGaIn/GaN HEMT devices,” *IEEE Trans. Electron Devices*, vol. 54, no. 3, pp. 410-417, March 2007.

[8] S. Russo and A. D. Carlo, “Influence of the source-gate distance on the AlGaIn/GaN HEMT performance,” *IEEE Trans. Electron Devices*, vol. 54, no. 5, pp. 1071-1075, May 2007.

[9] J. C. Zhang, P. T. Zheng, Z. D. Dong, *et al.*, “The Effect of Back-barrier Layer on the Carrier Distribution in the AlGaIn/GaN Double-hetero Structure,” *Acta Physica Sinica*, vol. 58, no. 5, pp. 3409-3415, May 2009.

[10] M. Farahmand, C. Garetto, E. Bellotti, K. F. Brennan, *et al.*, “Monte Carlo simulation of electron transport in the III-nitride wurtzite phase materials system: Binaries and ternaries,” *IEEE Trans. Electron Devices*, vol. 48, no. 3, pp. 535-542, March 2001.

[11] J. C. Zhang, X. H. Ma, Y. Hao, L. Fan, and P. X. Li, “An analytic low field electron mobility model of wurtzite GaN,” *Journal of Semiconductors*, vol. 24, no. 10, pp. 1044-1048, October 2003.

[12] T. Nanjo, A. Imai, Y. Suzuki, Y. Abe, *et al.*, “AlGaIn channel HEMT with extremely high breakdown voltage,” *IEEE Trans. Electron Devices*, vol. 60, no. 3, pp. 1046-1053, March 2013.

[13] B. Du, J. L. Hudgins, E. Santi, A. T. Bryant, P. R. Palmer, and H. A. Mantooth, “Transient electrothermal simulation of power semiconductor devices,” *IEEE Trans. Power Electronics*, vol. 25, no. 1, pp. 237-248, January 2010.

[14] H. Q. Zhang and K. M. Huang, “Numerical simulation of the influence of high power electromagnetic pulses on GaAs mesfet,” *High Power Laser and Particle Beams*, vol. 18, no. 11, pp. 1873-1878, November 2006.

[15] D. Denis, C. M. Snowden, and I. C. Hunter, “Coupled electrothermal, electromagnetic, and physical modeling of microwave power fets,” *IEEE Trans. Microw. Theory & Tech.*, vol. 54, no. 6, pp. 2465-2470, June 2006.



Xiaobin Luo, born in 1983, Ph. D. candidate. He is the corresponding author of this paper. His research interests include GaN physical modeling, device electromagnetic-thermal coupling and GaN MMIC design.



Weihua Yu, received the B.S. degree in Radio Technology in 2000 and Ph.D. degree in Electromagnetic Field and Microwave Technology in 2005 from Beijing Institute of Technology, China. Now she is working at Beijing Institute of Technology. Her research interests include integrated circuit and system design at millimeter-wave and terahertz band.



Xin Lv, received the B.S. degree in 1982 and Ph.D. degree in 1993 in Electromagnetic Field and Microwave Technology from Beijing Institute of Technology, China. Now he is working at Beijing Institute of Technology. His research interests include integrated circuit and system design at millimeter-wave and terahertz band.